

**Time-varying earthquake occurrence in
Canterbury following the Darfield earthquake**

D. A. Rhoades
A. Christophersen

M. C. Gerstenberger

GNS Science Consultancy Report 2011/22
February 2011

DISCLAIMER

This report has been prepared by the Institute of Geological and Nuclear Sciences Limited (GNS Science) exclusively for and under contract to Earthquake Commission. Unless otherwise agreed in writing by GNS Science, GNS Science accepts no responsibility for any use of, or reliance on any contents of this Report by any person other than Earthquake Commission and shall not be liable to any person other than Earthquake Commission, on any ground, for any loss, damage or expense arising from such use or reliance.

The data presented in this Report are available to GNS Science for other use from February 2011.

BIBLIOGRAPHIC REFERENCE

Rhoades, D.A.; Gerstenberger, M.C.; Christophersen, A. 2010. Time-varying earthquake occurrence in Canterbury following the Darfield earthquake, *GNS Science Consultancy Report 2011/22*. 16 p.

CONTENTS

EXECUTIVE SUMMARY	ii
1.0 INTRODUCTION	3
2.0 EXPECTED NUMBER OF AFTERSHOCKS	4
3.0 STEP MODEL FORECAST	7
4.0 EEPAS MODEL FORECAST	9
5.0 CONCLUSION	14
6.0 ACKNOWLEDGEMENTS	14
7.0 REFERENCES	14

FIGURES

Figure 1	Weekly forecasts of four aftershock models applied to the Darfield earthquake, and the observations from Monday 6 September until Monday 31 January.	6
Figure 2	Cumulative weekly forecasts of four aftershock models applied to the Darfield earthquake, and the observations from Monday 6 September until Monday 31 January.	6
Figure 3	Log number of events forecast for the period July 1, 2011 to June 30, 2012 from the STEP model. For the total aftershock sequence 22.9 M \geq 4 earthquakes are forecast during the time period.	8
Figure 4	Example of the precursory scale increase phenomenon for the 1989 M7.0 Loma Prieta, California, (a) Precursor area (dashed rectangle) showing locations of precursory earthquakes, mainshock and aftershocks; (b) Magnitude vs time plot, showing mainshock magnitude M_m , precursor magnitude M_p and increase in magnitude level at onset of precursors in 1979 (dashed line); (c) Cumulative magnitude anomaly (Cumag) vs time, showing change of slope at onset of precursors. The protractor relates slopes of the cumag to the rate of earthquake occurrence in magnitude units per year above the minimum magnitude plotted (4.0). A negative slope indicates a below-average rate and a positive slope an above-average rate of earthquake occurrence within the period covered by the plot. The Cumag plot ends just before the mainshock; a separate cumag plot covers the period of the mainshock and aftershocks.	9
Figure 5	Predictive scaling relations derived from many examples of the precursory scale increase phenomenon. (a) Mainshock magnitude M_m vs precursor magnitude M_p ; Precursor time T_p versus M_p ; (c) Precursor area A_p versus M_p . The EEPAS model regards every earthquake as a long-range precursor of larger earthquakes and applies these relations to derive the contribution from each individual earthquake, according to its magnitude, to the future hazard.	10
Figure 6	Normalised earthquake occurrence rate at magnitude 5.0 under the EEPAS model for the year beginning 1 July 2011. The forecast is normalised relative to a reference (RTR) model in which 1 earthquake per year is expected exceeding any magnitude m in an area of 10^m km ²	12
Figure 7	Normalised earthquake occurrence rate at magnitudes 5.5 – 8.0 in steps of 0.5, under the EEPAS model for the year beginning 1 July 2011. The forecasts are normalised relative to a reference (RTR) model in which 1 earthquake per year is expected exceeding any magnitude m in an area of 10^m km ²	13

TABLES

Table 1	The model parameters used in the modified Omori law.	5
Table 2	Forecasts of magnitude 4 and larger aftershocks in the time period 1 July 2011 until 30 June 2012, and their 95% Poisson confidence bounds.	5
Table 3	Vertices of a polygon enclosing the Darfield aftershocks and used for the fitting of the sequence-specific model.	7

EXECUTIVE SUMMARY

We present one year earthquake forecasts in the Canterbury region for the year 1 July 2011 to 30 June 2012, using three approaches. First we estimate the expected total number of aftershocks of the 4 September 2010 earthquake based on the Omori-Utsu law for aftershock decay and the Gutenberg-Richter frequency-magnitude relation. Secondly we produce forecasts using two well-studied models installed in the New Zealand earthquake forecast testing centre, namely the Short-Term Earthquake Probability (STEP) model and the Every Earthquake a Precursor According to Scale (EEPAS) model, on a spatial grid in steps of 0.1 magnitude units.

Under the Omori-Utsu law with our preferred parameter estimates, 23.2 aftershocks of the Darfield earthquake with magnitude 4.0 or greater are expected to occur during the year, with a 95% Poisson confidence range between 14 and 33 aftershocks. In a wider Canterbury region, 22.9 earthquakes with magnitude 4.0 or greater are expected according to the STEP model, and 2.3 earthquakes with magnitude 5.0 or greater are expected according to the EEPAS model.

These estimates are based on data available in the GeoNet earthquake catalogue to 31 January 2011.

1.0 INTRODUCTION

The M7.1 Darfield earthquake of 4 September 2010, which occurred in a region of previously low seismicity, has brought about a marked increase in earthquake occurrence in the Canterbury region. The aftershock activity from this event is likely to continue for years, and to gradually subside according to the inverse power relation known as the Omori-Utsu law (Utsu *et al.* 1995).

It is possible that the stress changes resulting from this earthquake could trigger others in the medium term, and that some of the aftershocks could themselves be part of the preparation process of future major earthquakes in the region. Detailed seismological and geological studies of the mechanism of the Darfield earthquake and associated physical processes can currently provide qualitative information about hypotheses of the occurrence of future earthquakes; in time these studies may help to quantitatively refine future assessments of the potential for the Darfield earthquake sequence to trigger other major events in the region. In the meantime, there exist some standard statistical models which can be used to estimate the time-varying probability of future earthquake occurrences based only on the earthquake catalogue to date, including time-space aftershock models and medium-term forecasting models which make use of predictive relations derived from past earthquake sequences. In regional studies and tests around the globe, including New Zealand, these models have demonstrated predictive power and can provide quantitative estimates of expected earthquakes in the time following the Darfield main shock.

This report is concerned with the probability of earthquake occurrence in the Canterbury region during the one-year period from 1 July 2011 to 30 June 2012 and its distribution in space and magnitude. First, we estimate the expected total number of aftershocks of the 4 September 2010 based on the Omori-Utsu law for aftershock decay and the Gutenberg-Richter frequency-magnitude relation. Secondly, we estimate the expected number of earthquakes in space-magnitude bins from two standard models, which have been applied to several different regions and are currently being formally and transparently tested in the New Zealand testing centre of the Collaboratory for the study of Earthquake Predictability (CSEP). These models are the Short-Term Earthquake probability (STEP) model of Gerstenberger (2003) and the Every Earthquake a precursor According to Scale (EEPAS) model. Although these models have been tested in a number of ways by their authors, their performance in the transparent formal tests is unknown at this point, because of periods of incompleteness in the catalogue necessary for the tests.

These estimates are based on data available in the GeoNet earthquake catalogue to 31 January 2011. The STEP and EEPAS models assume the catalogue to be substantially complete down to magnitude 3 in recent years. However, this condition is known not to be completely met. There is a period of more than eight months between mid 2007 and mid 2008 for which the catalogue has still to be finalised, and is known to be not yet complete down to magnitude 3. There are also shorter periods of incompleteness during the aftershock sequences of several recent major events. In particular, and what is most important for this study, the cataloguing of the early aftershocks on the first day following the Darfield main shock is not yet complete. These catalogue deficiencies inevitably affect the estimates presented to some degree, but probably not in a major way.

2.0 EXPECTED NUMBER OF AFTERSHOCKS

The Omori-Utsu law is the oldest empirical relationship in seismology and originally described how the number of felt aftershocks per day decayed with time t as $1/t$ for the 1891 Nobi, Japan earthquake (Omori, 1894). The relationship was found to still be ongoing 100 years after the Nobi earthquake (Utsu *et al.*, 1995). Equation (1) shows the modified version of the original relationship with an additional parameter p that controls the temporal decay.

$$n(t) = \frac{K}{(t+c)^p}, \quad (1)$$

The parameter K represents the productivity. The meaning of the constant c is still being debated (e.g. Enescu *et al.*, 2009; Narteau *et al.*, 2009) but its presence allows for a time delay between mainshock and the onset of the power law decay. This delay is either due to physical properties, network properties, or both. In case of the Darfield earthquake we are not certain, that all aftershocks of magnitude 4 and above are detected and reported in the GeoNet catalogue within the first couple of days following the mainshock. This is partly due to smaller events being wrapped within the coda of larger events, and partly due to lack of resources to do more detailed analysis.

Reasenbergs and Jones (1989) fitted the parameters of the modified Omori law for 62 sequences in California and derived an average relationship for K .

$$K = 10^{a'+b(M_m-M_0)}, \quad (2)$$

where a' is an average productivity constant, b is the b -value of the magnitude-frequency distribution of aftershocks, M_m the mainshock magnitude and M_0 the magnitude of the smallest aftershocks of interest. The method was applied to New Zealand by Eberhart-Phillips (1998) with similar parameters for California, although with a wide variation between sequences. Both earlier applications of the Reasenbergs-Jones model only used aftershock sequences that had sufficient data to have their parameters fitted, neglecting smaller sequences. An update of the Reasenbergs-Jones model for New Zealand also includes information from stacked smaller sequences (Pollock, 2007). The average parameters are similar and are given in Table 1.

Recently, we have developed an alternative estimate for the average K -value, based on the observed number of aftershocks per sequence. This is called the mean abundance model (Christophersen & Gerstenberger, 2010). Table 1 compares the parameters for both methods for a magnitude $M=7.1$ earthquake in New Zealand. The table also includes the b -value of the magnitude-frequency relation that was found for each model. In addition we fitted the parameters b , K , p , and c for the Darfield aftershock sequence and also include them in the Table 1.

We use all three models, as well as the specific parameters to forecast the number of magnitude 4 and larger aftershocks in the time period 1 July 2011 until 30 June 2012. To fit the sequence specific parameters we need a complete set of aftershock. Most aftershocks occur immediately following the mainshock when the magnitude threshold for detecting smaller events is low. The data for the fitting was selected from a polygon around the fault with vertices as in Table 3. Fitting the completeness magnitude with time suggests that aftershocks of magnitude 3 are not completely detected within the first week when the most

active period is past. We fitted the parameters to aftershocks of magnitude 4 and larger and varied the starting period of the fit from 0 (170 earthquakes in data set) to 2.5 days (106 earthquakes in data set) in 0.1 day steps. From 1.5 days the estimated parameters do not change significantly. The parameters shown in Table 1 correspond to 1.8 days after the mainshock, which is Monday, 6 September 2010, 0:00 a.m. The fitted data set includes 113 earthquakes, only one less than when fitting from 1.5 days. As a consequence of the small number of data fitted, the standard errors of the parameters are quite large. Therefore we prefer the forecasts of the mean abundance model

The forecast mean values for the four models and the 95% Poisson confidence intervals are displayed in Table 2. Figure 1 shows a cumulative plot of the four models and the weekly observations of magnitude 4 and larger aftershocks until the end of January. The grey lines are the 95% confidence limits of the mean abundance model. As expected, the sequence specific model fits the data best as it is derived from all the data displayed. The data fall within the 95% Poisson range of the mean abundance model, while the Reasenber-Jones type models both overpredict the aftershock occurrence for the previous period. Due to a larger p -value than the mean abundance model, the forecast for the Reasenber-Jones (Pollock) model over the one year period starting 1 July is very similar to that of the mean abundance model.

Under the Omori-Utsu law with our preferred parameter estimates, 23.2 aftershocks of the Darfield earthquake with magnitude 4.0 or greater are expected to occur during the year, with a 95% Poisson confidence range between 14 and 33 aftershocks. The mean forecasts of the other models fall within this range.

Table 1 The model parameters used in the modified Omori law.

Model	b -value	K -value for $M=7.1$	p -value	c -value
Reasenber & Jones (Eberhart-Phillips)	1.03 (median)	38.4	1.02 (median)	0.03 (median)
Reasenber & Jones (Pollock)	1.03 (median)	45.1	1.07 (median)	0.04 (median)
Mean Abundance	1.0 (fixed)	26.0	1.0 (fixed)	0.1 (fixed)
Sequence specific for $M \geq 4$ aftershocks from day 1.8	0.96±0.18	32.0±23.1	1.05±0.18	0.69±1.96

Table 2 Forecasts of magnitude 4 and larger aftershocks in the time period 1 July 2011 until 30 June 2012, and their 95% Poisson confidence bounds.

Model	Average Forecast	Lower Poisson 95% bound	Higher Poisson 95% bound
Reasenber & Jones (Eberhart-Phillips)	27.1	17	38
Reasenber & Jones (Pollock)	23.4	14	33
Mean Abundance	23.2	14	33
Sequence specific for $M \geq 4$ aftershocks from day 1.8	18.9	11	28

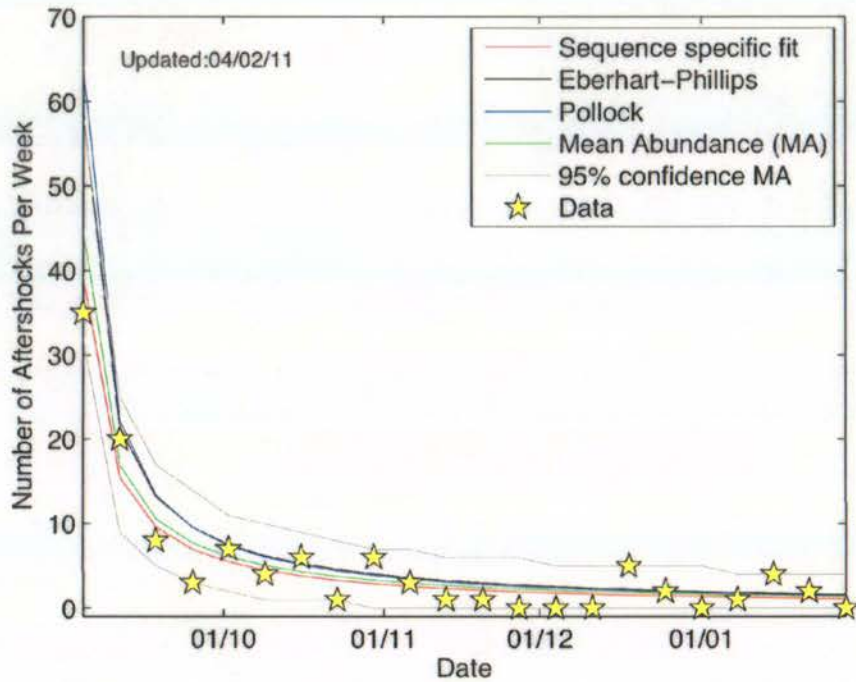


Figure 1 Weekly forecasts of four aftershock models applied to the Darfield earthquake, and the observations from Monday 6 September until Monday 31 January.

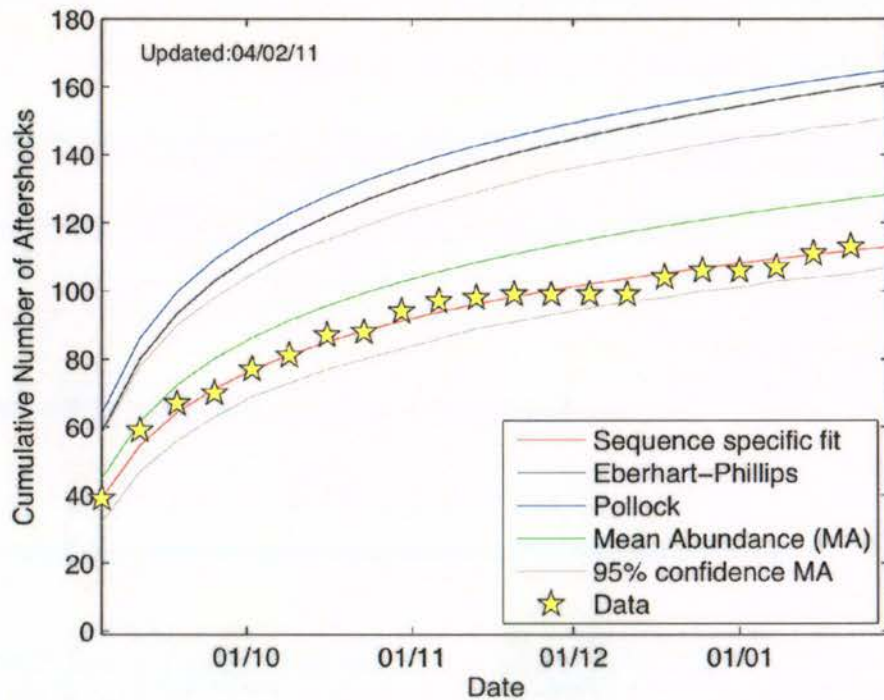


Figure 2 Cumulative weekly forecasts of four aftershock models applied to the Darfield earthquake, and the observations from Monday 6 September until Monday 31 January.

Table 3 Vertices of a polygon enclosing the Darfield aftershocks and used for the fitting of the sequence-specific model.

Longitude	Latitude
171.33	-43.64
171.78	-42.82
172.39	-42.88
173.08	-43.20
173.45	-43.61
173.35	-43.97
172.66	-44.31
171.66	-44.07
171.33	-43.64

3.0 STEP MODEL FORECAST

The STEP (Short-Term Earthquake Probability; Gerstenberger *et al.*, 2004, 2005) model is an aftershock model based on the idea of superimposed Omori (Ogata, 1988, 1998) type sequences. The model is comprised of two components: 1) a background model; and 2) a time-dependent clustering model. The background model can consist of any model that is able to forecast a rate of events for the entire region of interest at all times; for the forecasts provided here, either the 2002 (Stirling *et al.*, 2002) NZ National Seismic Hazard Model, or a zero-rate model is used as the background model (i.e. the background model is ignored). The clustering model is described based on the work of Reasenber & Jones (1989) which defines aftershock forecasts based on the a - and the b - value from the Gutenberg-Richter relationship (Gutenberg & Richter, 1954) and the p -value from the modified Omori law (Ogata, 1988, 1998). The STEP model defines these aftershock forecasts based on three model-components. The first component is based on the average behaviour of aftershocks in New Zealand and uses the median Reasenber and Jones parameter values for New Zealand aftershocks, as estimated by Pollock (2007). The second component uses the development of the ongoing aftershock sequence to attempt to improve the information in the forecast. In this component the Reasenber and Jones parameters are estimated for each individual aftershock sequence as it develops. The third component allows for spatial heterogeneities within the sequence by calculating the Reasenber and Jones parameters on a 0.1 degree by 0.1 degree grid within the aftershock sequence. The second and third components are only practical for large aftershock sequences with more than 100 aftershocks above the threshold of completeness; therefore, in practice, the STEP forecasts are typically dominated by the first component. In order to produce a single forecast based on the three component forecasts, each forecast is weighted by a score from the corrected Aikake Information Criterion (AICc; Burnham & Anderson, 2002) and the three weighted forecasts are summed. The AICc is based on a model's likelihood score, the amount of data and the number of free parameters that must be estimated, thus ensuring a smooth transition from the generic component to the spatially-heterogeneous component as more data becomes available. Finally, for each grid node, all aftershock forecasts are compared to the background forecast for the node and the highest forecast is retained.

The spatial distribution of the forecast aftershocks is partially decoupled from the rate calculation. The rate forecast is isotropically distributed using a radius based on the subsurface rupture length from Wells and Coppersmith (1994) and using a $1/r^2$ taper. If the radius is less than the grid spacing, a point source is assumed and the rates are smoothed in a circular fashion using the $1/r^2$ taper; otherwise a two segment fault is estimated based on the density of the aftershock distribution and the rates are smoothed using the $1/r^2$ taper from the fault. Additionally, because each aftershock can generate its own rate forecast as well as contributing to the overall rate forecast of the main shock, spatial heterogeneities are added by superimposing individual aftershock forecasts on the main shock forecast. When more than one forecast is calculated for a single grid node, only the largest forecast is retained.

The forecast as calculated for the Darfield sequence for the time period July 1st, 2011 to June 30, 2012 is shown in Figure 3. In this time period 22.9 $M \geq 4$ events are forecast for the aftershock sequence. In the figure, the east-west strike of the fault as automatically estimated by the aftershock distribution is apparent by the increased rates along this feature (red colours). The decay in rates is largely isotropic with the only off-fault increase in rates occurring at the north-east end of the fault. Outside of the aftershock zone, multiple small rate increases can be seen that are caused by increased activity out of the immediate aftershock zone. Additionally, the background trend from the National Seismic Hazard Model of increased rates around the Alpine Fault can be seen in the lighter blue colours.

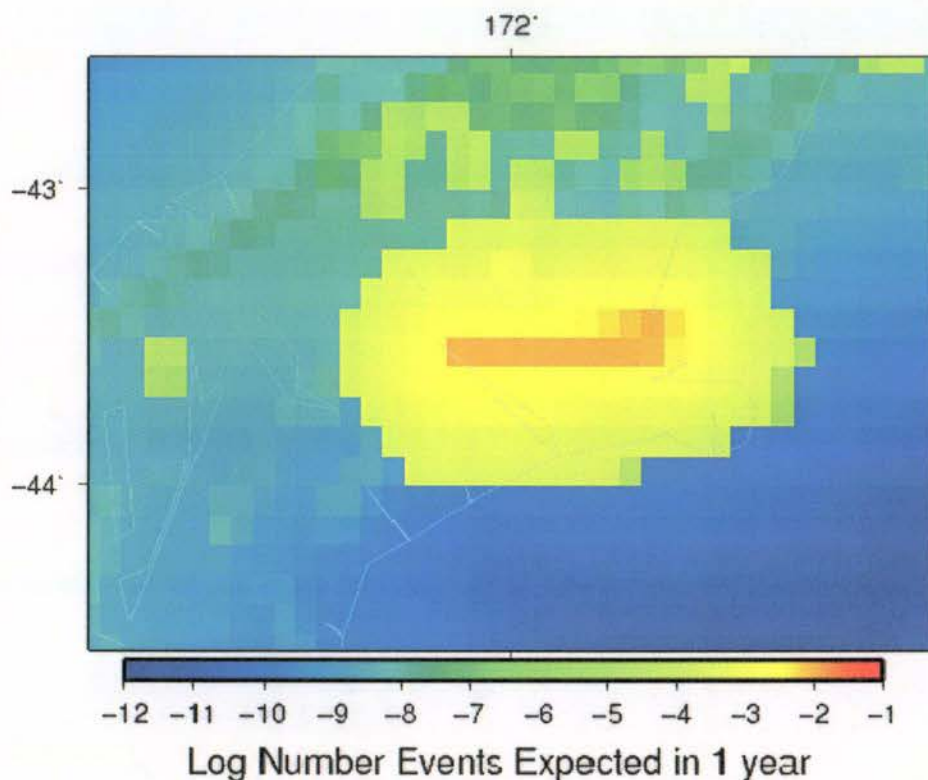


Figure 3 Log number of events forecast for the period July 1, 2011 to June 30, 2012 from the STEP model. For the total aftershock sequence 22.9 $M \geq 4$ earthquakes are forecast during the time period.

4.0 EEPAS MODEL FORECAST

The EEPAS model (Rhoades and Evison, 2004) is a long-range earthquake forecasting model based on the precursory scale increase phenomenon and associated predictive relations (Evison and Rhoades, 2002; 2004). The precursory scale increase is an increase in the magnitude and rate of occurrence of minor earthquakes which typically precedes most major earthquakes in the long term (Figure 4). The predictive scaling relations are linear regressions of mainshock magnitude, log precursor time and log precursor area on precursor magnitude (Figure 5).

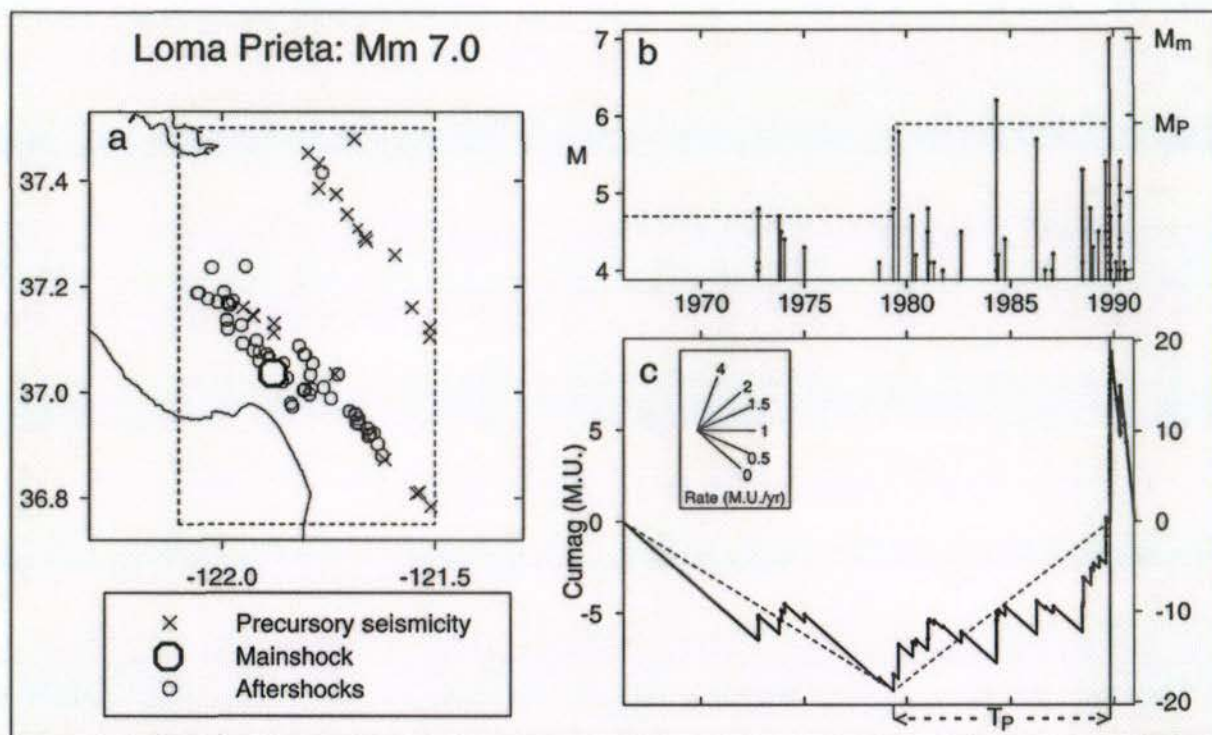


Figure 4 Example of the precursory scale increase phenomenon for the 1989 M7.0 Loma Prieta, California, (a) Precursor area (dashed rectangle) showing locations of precursory earthquakes, mainshock and aftershocks; (b) Magnitude vs time plot, showing mainshock magnitude M_m , precursor magnitude M_p and increase in magnitude level at onset of precursors in 1979 (dashed line); (c) Cumulative magnitude anomaly (Cumag) vs time, showing change of slope at onset of precursors. The protractor relates slopes of the cumag to the rate of earthquake occurrence in magnitude units per year above the minimum magnitude plotted (4.0). A negative slope indicates a below-average rate and a positive slope an above-average rate of earthquake occurrence within the period covered by the plot. The Cumag plot ends just before the mainshock; a separate cumag plot covers the period of the mainshock and aftershocks.

The EEPAS model assumes that the precursory scale increase occurs at all scales in the seismogenic process. It sets aside any attempt to distinguish precursory earthquakes from others, and simply regards every earthquake as a precursor of larger events to follow it in the medium-to-long term. Each precursor makes a transient contribution to the estimate of future earthquake occurrence in its surroundings. The magnitude distribution of that contribution is centred at about one unit higher than the magnitude of the precursor (Figure 5a). The mean of the time distribution increases with the magnitude of the precursor as shown in Figure 4b. For example, the contribution from a magnitude 4 earthquake peaks 2-3 years after its

occurrence. The spatial distribution of the contribution occupies an area that increases with the magnitude of the precursor as shown in Figure 4c.

For full details of the model, see Rhoades and Evison (2004).

The model makes no attempt to estimate aftershocks following the Omori-Utsu law. It is aimed at long-range forecasting of major earthquakes and is concerned solely with the possibility that small earthquakes may be precursory to larger ones. A linear combination of the STEP and EEPAS models has been found to be more informative as a short-term forecasting model than either of these models by themselves (Rhoades and Gerstenberger, 2009), with a combination of $0.42 \times \text{EEPAS} + 0.58 \times \text{STEP}$ being optimal for California.

There is evidence that an individual earthquake can be both an “aftershock” and a “precursor” at the same time. For example, some of the aftershocks of the 1992 Landers, California, M7.3, earthquake participated in the precursory scale increase associated with the 1999 Hector Mine M7.1 earthquake (Evison and Rhoades, 2004b).

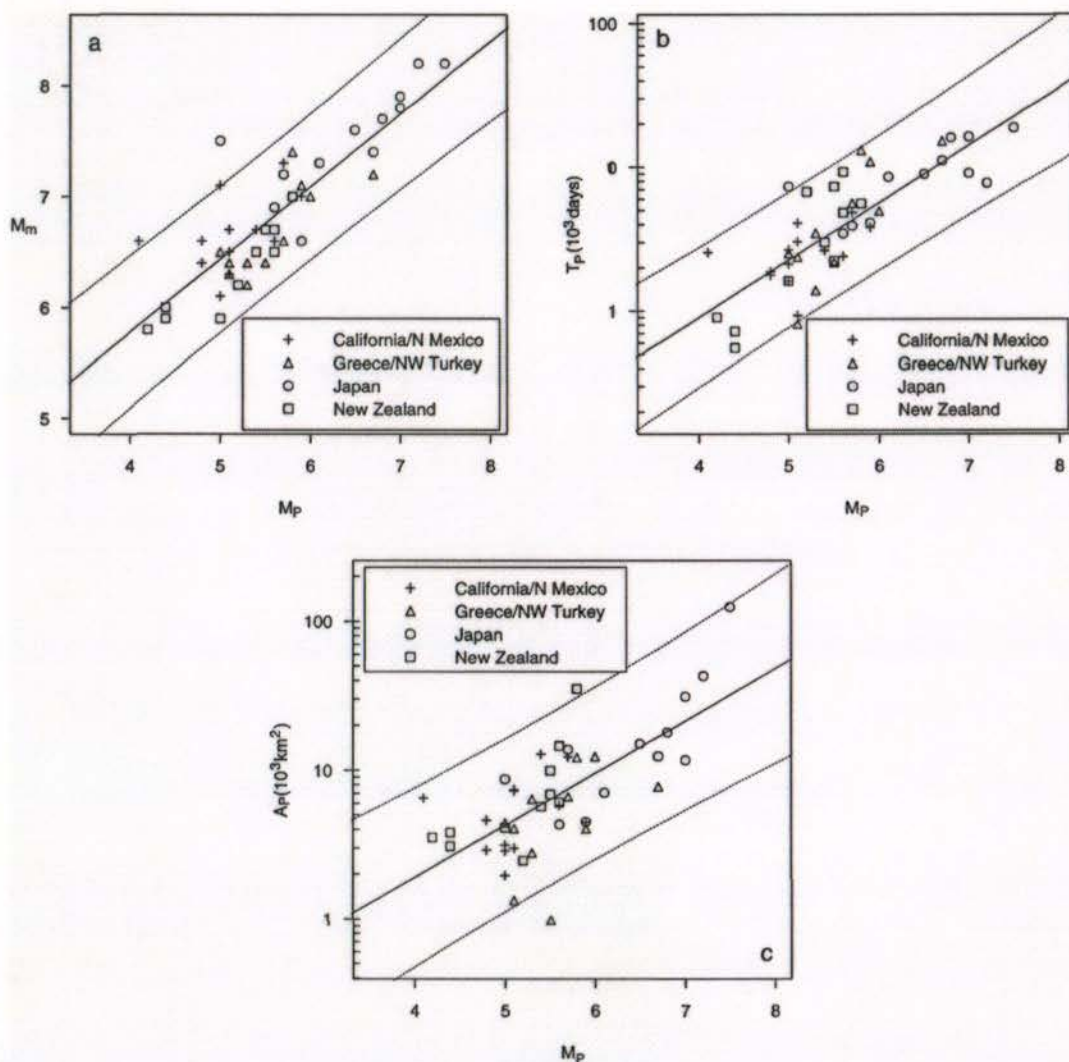


Figure 5 Predictive scaling relations derived from many examples of the precursory scale increase phenomenon. (a) Mainshock magnitude M_m vs precursor magnitude M_p ; Precursor time T_p versus M_p ; (c) Precursor area A_p versus M_p . The EEPAS model regards every earthquake as a long-range precursor of larger earthquakes and applies these relations to derive the contribution from each individual earthquake, according to its magnitude, to the future hazard.

In past studies, the EEPAS model has been applied to New Zealand and California at a magnitude threshold $m_c = 5.75$, to Japan with $m_c = 6.75$ and 6.25 , to the Kanto region in central Japan with $m_c = 4.75$, to Greece with $m_c = 5.95$; and to southern California with $m_c = 4.95$ (Rhoades and Evison, 2004, 2005, 2006; Console et al., 2006; Rhoades, 2007). In the New Zealand earthquake forecast testing centre, the magnitude threshold is $m_c = 4.95$ and catalogue completeness down to magnitude 3.0 is assumed. Four different versions of the model are being tested, but here we present the forecasts from the version that gives the best fit to the past catalogue. In this version all earthquakes are weighted equally, and the full set of model parameters are fitted to the New Zealand catalogue. The model is a linear combination of a time-varying component based on the predictive relations and a background spatially smoothed seismicity model. In most applications the background contribution is found to be small, as in the present case in which it contributes about 5% of the total hazard.

The EEPAS model forecast for the year beginning 1 July 2011, using GeoNet catalogue data up to 31 January 2010, is illustrated in Figures 6 and 7. The total expected number of earthquakes exceeding magnitude 4.95 within the region plotted is 2.25. Figure 6 illustrates the spatial distribution of the expected earthquake rate for magnitude 5.0. The EEPAS forecasts do not necessarily follow the Gutenberg-Richter frequency-magnitude law at given times and locations. Therefore the spatial distribution can change with magnitude. Figure 7 shows comparable plots of the spatial distribution for magnitudes up to 8.0 at intervals of 0.5. The earthquake rate is normalized relative to a reference model with Gutenberg-Richter b-value of 1. If the forecasts followed the Gutenberg-Richter law with a b-value slope of 1, all of these plots would be identical. What these plots show is that, relative to the reference model, the rate progressively decreases in the Darfield area as magnitude increases above about M 7.0. This can partly be explained by the scaling relations for magnitude and precursor time (Figure 5). According to these relations, the contribution of the smaller aftershocks to the long-term hazard (which is concentrated at relatively low target magnitudes, about 1-2 units larger than the aftershocks themselves) peaks sooner than that of the larger aftershocks and the main shock (at higher magnitudes).

No precursory scale increase for the Darfield earthquake can be seen in the earthquake catalogue. There is evidence from published studies on regional earthquake catalogue (Rhoades and Evison 2004, 2005, 2006; Rhoades, 2007, 2009) and from current research on global catalogues that the precursor time may increase with the local seismicity rate (or local crustal strain rate). The Greendale fault that ruptured in the Darfield earthquake is in a low strain rate region. Therefore we may expect that the precursor time for a magnitude 7.1 in this region could be over 100 years rather the 10-15 years that would be expected in higher strain-rate regions. In that case, it might not be seen at all in the instrumental catalogue. In that case also, the time distribution of the EEPAS model as applied here would be too short; the model would overestimate the contribution from the Darfield aftershocks to the expected earthquake occurrence in the year beginning 1 July 2011, and miss out altogether on contributions from earthquakes that occurred prior to the start of the catalogue used here (1950).

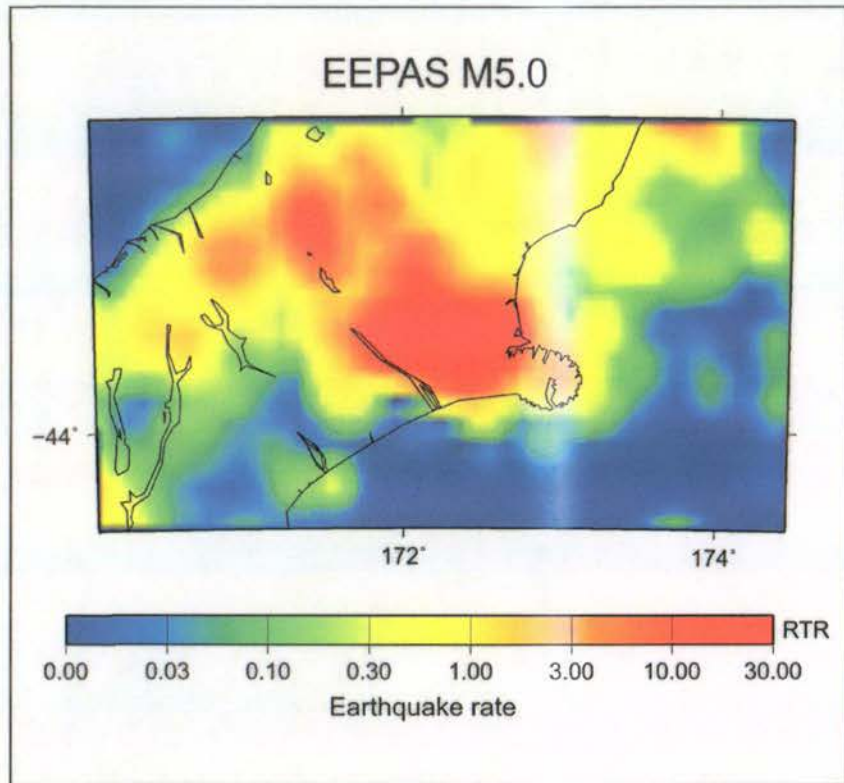


Figure 6 Normalised earthquake occurrence rate at magnitude 5.0 under the EEPAS model for the year beginning 1 July 2011. The forecast is normalised relative to a reference (RTR) model in which 1 earthquake per year is expected exceeding any magnitude m in an area of 10^m km^2 .

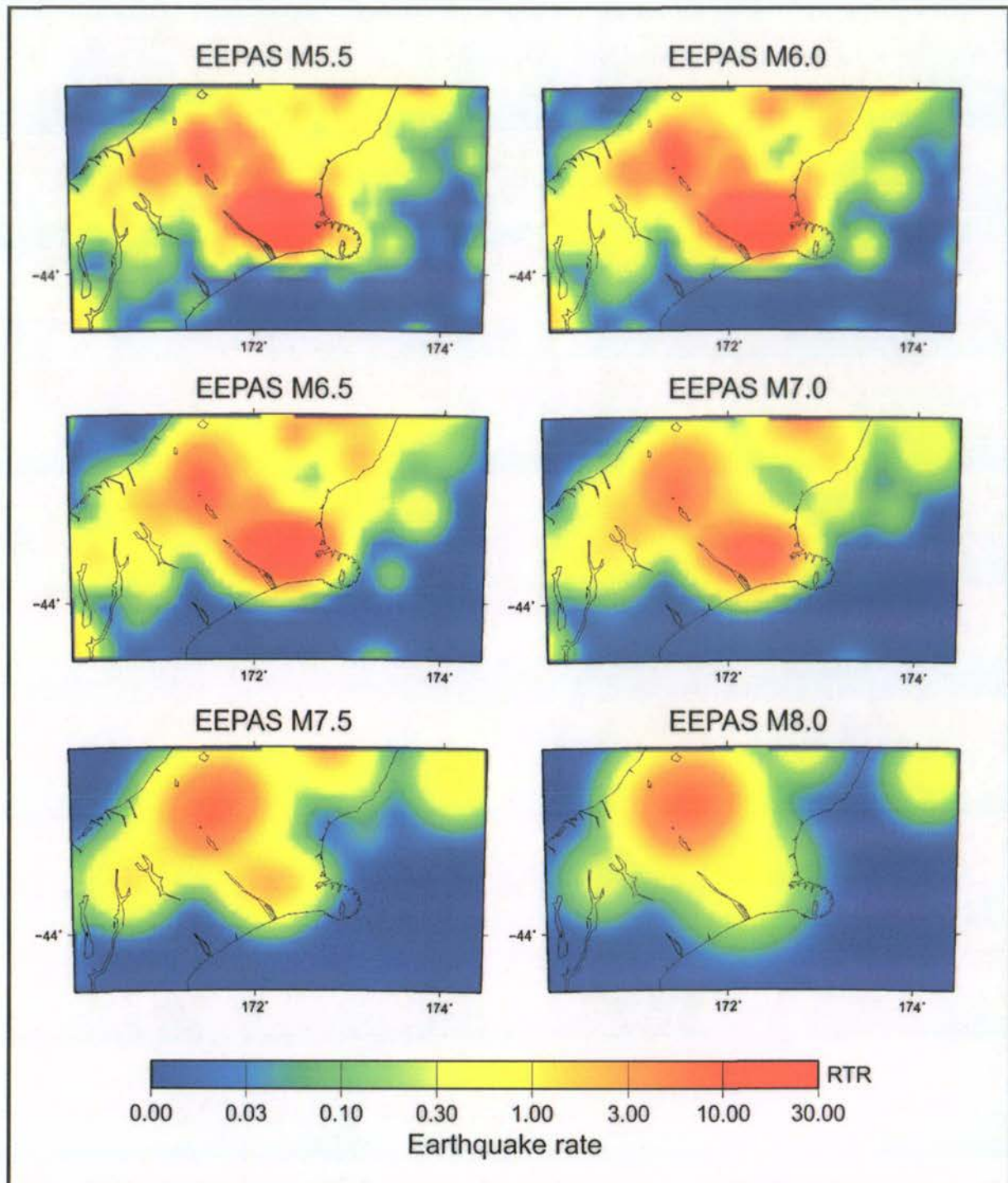


Figure 7 Normalised earthquake occurrence rate at magnitudes 5.5 – 8.0 in steps of 0.5, under the EEPAS model for the year beginning 1 July 2011. The forecasts are normalised relative to a reference (RTR) model in which 1 earthquake per year is expected exceeding any magnitude m in an area of 10^m km^2 .

5.0 CONCLUSION

According to the Omori-Utsu law with our preferred parameter estimates, 23.2 aftershocks of the Darfield earthquake with magnitude 4.0 or greater are expected to occur during the year commencing 1 July 2011, with a 95% Poisson confidence range between 14 and 33 aftershocks. In a wider Canterbury region, 22.9 earthquakes with magnitude 4.0 or greater are expected according to the STEP model, and 2.3 earthquakes with magnitude 5.0 or greater are expected according to the EEPAS model.

These estimates are broadly consistent with each other. However, the STEP and EEPAS models differ in the detail of their spatial and magnitude distributions. Such differences are only to be expected, because the STEP model is concerned with aftershocks and the EEPAS model with the long-term seismogenic process for major earthquakes.

6.0 ACKNOWLEDGEMENTS

This report has been internally reviewed by Robert Buxton and Caroline Holden.

7.0 REFERENCES

- Burnham; K. P. and Anderson; D. R. (2002) Model Selection and Multimodel inferences A Practical Information-Theoretic Approach, 488, Springer, New York.
- Christophersen; A. and Gerstenberger; M. C. (2010). A new generic model for aftershock occurrence. *Bulletin of the Seismological Society of America*, **submitted**.
- Eberhart-Phillips; D. (1998). Aftershock sequence parameters in New Zealand. *Bull. Seism. Soc. Am.*, **88**, 1095-1097.
- Enescu; B., Mori; J., Masatoshi; M. and Yasuyuki; K. (2009). Omori-Utsu law c-values associated with recent moderate earthquakes in Japan. *Bulletin of the Seismological Society of America*, **99**(2a), 884-891.
- Evison; F. F. and Rhoades; D. A. (2004). Demarcation and scaling of long-term seismogenesis. *Pure and Applied Geophysics* **161**, 21-45.
- Evison; F. F. and Rhoades; D. A., (2004b). Long-term seismogenesis and self-organized criticality. *Earth Planets and Space*, **56**, 749-760.
- Gerstenberger; M. C. (2003). Earthquake clustering and time-dependent probabilistic seismic hazard analysis for California. *Dissertation submitted to the Swiss Federal Institute of Technology for the degree of Doctor of Science, Zurich*.
- Gerstenberger; M. C., Wiemer; S. and Jones; L. (2004). Real-time forecasts of tomorrow's earthquakes in California: a new mapping tool. Denver, Colo., *U.S. Geological Survey. Open-file report 2004-1390*. 390p.

- Gerstenberger; M., Wiemer; S., Jones; L. M. and Reasenber; P. A. (2005). Real-time forecasts of tomorrow's earthquakes in California, *Nature* **435**, 328-331.
- Gutenberg; B. and Richter; C. F. (1954) Seismicity of the Earth and Associated Phenomena, 2nd ed. Princeton, N.J.: Princeton University Press, pages 17–19.
- Narteau; C., Byrdina; S., Shebalin; P., & Schorlemmer; D. (2009). Common dependence on stress for the two fundamental laws of statistical seismology. *Nature*, **462**(7273), 642-645.
- Omori; F. (1894). On aftershocks. *Report of Imperial Earthquake Investigation Committee*, **2**, 103-109.
- Ogata; Y. (1988), Statistical models for earthquake occurrences and residual analysis for point processes, *Journal of American Statistical Association*, **83**, 9-27.
- Ogata; Y. (1998). Space-time point process models for earthquake occurrences. *Annals of the Institute. Statistical Mathematics* **50**, 379–402.
- Pollock; D. (2007). *Aspects of short-term and long-term seismic hazard assessment in New Zealand*. Diploma Thesis, Institute of Geophysics, ETH, Zurich, Switzerland.
- Reasenber; P. A. and Jones; L. M. (1989) Earthquake hazard after a mainshock in California, *Science* **243**, 1173-1176.
- Rhoades; D. A. (2007) Application of the EEPAS model to forecasting earthquakes of moderate magnitude in southern California. *Seismological Research Letters* **78** (1), 110-115.
- Rhoades; D. A. (2009). Long-range earthquake forecasting allowing for aftershocks. *Geophysical Journal International*, **178**, 244-256.
- Rhoades; D. A. and Evison; F. F. (2004). Long-range earthquake forecasting with every earthquake a precursor according to scale. *Pure and Applied Geophysics* **161**, 47–71.
- Rhoades; D. A. and Evison; F. F. (2005). Test of the EEPAS forecasting model on the Japan earthquake catalogue. *Pure and Applied Geophysics* **162**, 1271–1290.
- Rhoades; D. A. and Evison; F. F. (2006). The EEPAS forecasting model and the probability of moderate-to-large earthquakes in the Kanto region, central Japan. *Tectonophysics* **417**, 119-130.
- Rhoades; D. A. and Gerstenberger; M. C. (2009). Mixture models for improved short-term earthquake forecasting. *Bulletin of the Seismological Society of America* **99**, 636-64.
- Stirling; M. W., McVerry; G. H. and Berryman; K. R. (2002). A new seismic hazard model for New Zealand. *Bull. Seismol. Soc. Amer.* **92**, 1878–1903.
- Utsu; T., Ogata; Y. and Matsu'ura; R. S. (1995). The centenary of the Omori formula for a decay law of aftershock activity. *Journal of the Physics of the Earth*, **43**, 1-33.
- Wells; D.L. and Coppersmith; K.J. (1994). New empirical relationships among magnitude, rupture length, rupture width, rupture area, and surface displacement. *Bull. Seismol. Soc. Am.* **84**, pp. 974–100.



www.gns.cri.nz

Principal Location

1 Fairway Drive
Avalon
Lower Hutt 5010
PO Box 30368
Lower Hutt 5040
New Zealand
T +64-4-570 1444
F +64-4-570 4600

Other Locations

Dunedin Research Centre
764 Cumberland Street
Dunedin 9016
Private Bag 1930
Dunedin 9054
New Zealand
T +64-3-477 4050
F +64-3-477 5232

Wairakei Research Centre
114 Karetoto Road, Wairakei
Taupo 3377
Private Bag 2000
Taupo 3352
New Zealand
T +64-7-374 8211
F +64-7-374 8199

National Isotope Centre
30 Gracefield Road, Gracefield
Lower Hutt 5010
PO Box 31312
Lower Hutt 5040
New Zealand
T +64-4-570 1444
F +64-4-570 4657